Optics Letters

3D-printed optics for laser materials processing

Leander Siegle,[1,*] Michael Wendt,[2] Dario Mekle,[2,3] Daniel Flamm,[2] and Harald Giessen[1,4]

[1] 4th Physics Institute and Research Center SCoPE, University of Stuttgart, Pfaffenwaldring 57, Stuttgart, 70569, Germany
[2] TRUMPF Laser- und Systemtechnik SE, Johannes-Maus Straße 2, Ditzingen, 71254, Germany
[3] Friedrich Schiller University Jena, Institute of Applied Physics, Abbe Center of Photonics, 07745, Jena, Germany
[4] giessen@pi4.uni-stuttgart.de
*l.siegle@pi4.uni-stuttgart.de

Received 25 May 2026; revised 17 July 2026; accepted 17 July 2026; posted 20 July 2026; published 3 August 2026

We report on high-power laser materials processing using 3D-printed beam shaping components. A diffractive axicon fabricated via two-photon polymerization is generating a Bessel-like beam for inducing in-volume modifications in transparent materials for cutting applications. The thin, centimeter-scaled, additively fabricated axicon structure is printed on a fused-silica substrate capable of withstanding average powers and peak intensities from an industrial ultrafast laser operating at 1 µm-wavelength. This concept enables fabrication of tailored beam shaping components for high-power laser applications within hours.

https://doi.org/10.1364/OL.606324

Laser-based materials processing has become state-of-the-art in modern manufacturing. Cutting, welding, texturing, additive manufacturing, etc. are enabled by the laser as a subtle, efficient, and non-contact tool for confined energy deposition that also allows for throughput scaling [1–3]. The technological scope extends equivalently across an expansive material spectrum—opaque or transparent alike—serving end products across e-mobility [4], consumer electronics [5], or the semiconductor industry [6]. It has recently become clear that the optics and the beam shaping concept provide a powerful lever to optimize established processes or even unlock entirely new ones [7–10]. However, realizing tailored optical functionality typically relies on customized components, such as diffractive or free-form optics, whose fabrication is time-consuming, leading to lead times of weeks to months. Here, we demonstrate a technique to additively manufacture centimeter-scale, customized beam-shaping components using two-photon polymerization, reducing fabrication time to just 10 hours. We further prove that these components withstand average and peak powers of an industrial high-power laser, and we validate their utility in a representative materials-processing experiment: precision cutting of glass enabled by an elongated focus distribution [11].

Maskless laser- or electron-beam lithography in fused silica represents the current state of the art for fabricating high-power-suitable diffractive optical elements (DOEs) with above- or sub-wavelength features, respectively, and overall dimensions of centimeters [5,7,12]. While these processes enable the production of high-precision DOEs with excellent efficiency and offer significant scalability through parallel manufacturing, the fabrication workflow—encompassing coating, exposure, development, etching, etc.—results in production cycles spanning several weeks. Production timelines can certainly be reduced significantly by increasing batch sizes and utilizing mask-based lithography to manufacture hundreds or thousands of identical elements. Nevertheless, research and development environments frequently require individual, custom elements. The high fabrication costs and complexity outlined above represent a significant barrier to DOE technology adoption.

Recently, Wahl *et al.* demonstrated a solution for rapid prototyping of reflective DOEs using laser-induced micro-delamination [13]. These structured mirrors accept high optical powers, operate in a broad wavelength range, and have proven their suitability for industrial use [13]. However, many optical designs necessitate transmissive solutions in particularly when it comes to high-NA focusing [14] or component rotation [11].

Additive manufacturing methods such as two-photon polymerization (2PP) for 3D printing transmissive (or reflective) optics, including DOEs, have become viable over the last few years, although typically slow and limited in overall size of the elements [15–19]. With the recent introduction of grayscale lithography to 2PP 3D printing [20,21], fabrication times of millimeter- or centimeter-sized optical structures with sub-micrometer features have decreased from days to hours [22–24]. However, so far, it has been used only in low-power applications [16,25–28].

Here, we overcome these power limitations by 3D-printing a micron-thick, square-centimeter-sized optically active layer on top of a fused-silica substrate. We investigate the fabrication, topography, optical performance, and glass cutting ability of a 2GL 3D-printed axicon DOE, with the aim of demonstrating rapid prototyping of optics for laser materials processing. We further demonstrate that the 3D-printed axicon DOE exhibits similar optical performance, in beam shaping and damage threshold, as a state-of-the-art diffractive axicon made of fused silica. The Bessel–Gaussian beam thus generated allows for single-pass, full-thickness cutting of display glasses

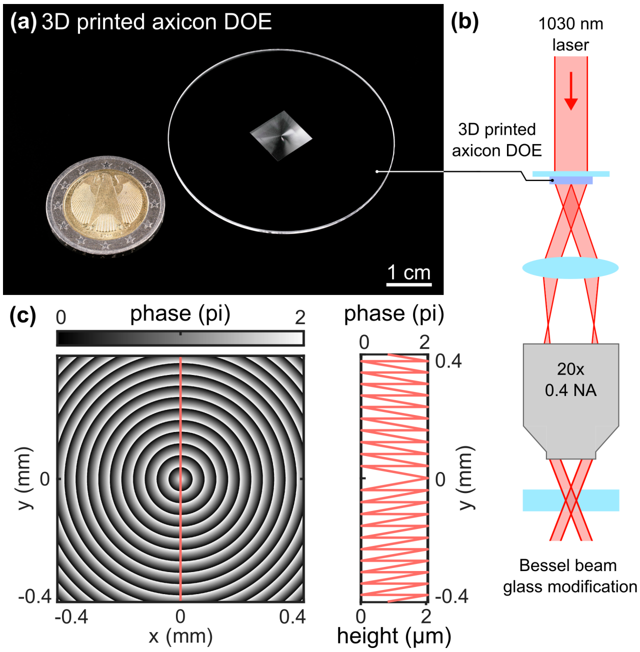

Fig. 1. 3D-printed axicon DOE with a size of 1 by 1 cm^2. (a) Overview of a two-inch wafer and a 2 Euro coin. (b) Schematic setup used for the modification of glass. (c) Designed phase distribution in the center of the axicon DOE highlighting the saw-tooth pattern with a cut-through along the *y*-axis.

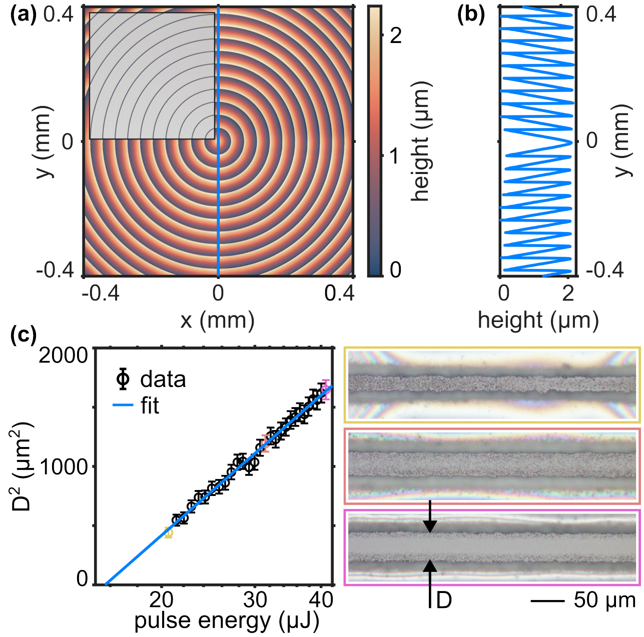

Fig. 2. (a) Central 800 × 800 µm^2 topography measured via confocal microscopy. The inset depicts a microscope top-view (Nikon Eclipse LV100ND with a 10×/0.30 NA objective). (b) *y*-profile through the center of the axicon along the solid line in (a). (c) Ablation fluence threshold measurements after the extended Liu method [31] plotting D^2 versus the laser pulse energy at a pulse length of 3ps and a repetition rate of 250 kHz. Here, D is the linewidth of the ablated line. The microscope images on the right correspond to the same-colored measurement points in the graph and highlight the width D.

with high edge qualities, as the corresponding elongated focus is length-adapted to the workpiece. The dimensions of the 3D-printed axicon DOE are highlighted in Fig. 1(a), confirming a clean diffractive surface and high optical transparency. Figure 1(b) schematically illustrates the optical setup used for glass modification.

A collimated laser beam of diameter 5 mm with a central wavelength of 1030 nm is illuminating the 3D-printed axicon DOE, generating the well-known interference pattern directly behind the axicon tip. Using the 4*f*-setup, the Bessel-Gaussian beam is imaged into the volume of the workpiece with a magnification of 20× [11]. The designed phase profile of said axicon DOE is depicted in Fig. 1(c). Here, only the central detail (800 × 800 µm^2) is shown to simplify assessment of the radially symmetric blazed grating and the axicon tip [7,29]. By design, an axicon with an opening angle of $\alpha = 3°$ is fabricated resulting in a phase distribution $\Phi(r) \approx \alpha r (n-1) 2\pi/\lambda$ and periods of $p \approx 40$ µm [7,29]. Equally to a lithographically fabricated element, for the 3D-printed axicon DOE, the phase Φ is produced through optical path length differences, requiring a height of $z = \lambda\Phi/[2\pi(n-1)]$ at a wavelength of λ and refractive index of the material of n [29]. Besides the exact realization of z_{max} to avoid large amounts of unmodulated light, high optical performance of DOEs requires excellent shape accuracy and sharp steps at the 2π-phase jumps. Moreover, a low surface roughness is required to minimize scattering losses. The axicon DOE is manufactured by two-photon polymerization grayscale lithography (2GL) using a Nanoscribe Quantum X (Nanoscribe GmbH Co. KG). Here, a femtosecond pulsed laser with a center wavelength of 780 nm and a repetition rate of 80 MHz is focused through a 25× magnification objective with NA of 0.8 (Zeiss LCI Plan-Neofluar 25×/0.80 Imm Korr DIC) into the photoresist Nanoscribe IP-S (Nanoscribe GmbH Co. KG, $n \approx 1.50$ at $\lambda = 1030$ nm [30]) which is deposited onto a two-inch diameter, 1 mm thick fused-silica wafer (JGS2 wafer, 2-side polished, MicroChemicals GmbH). Details of the 2GL 3D-printing process have been described in [18,24]. The key fabrication parameters are a slicing distance of 1 µm, a hatching distance of 0.2 µm, a scan speed of 200 mms^{-1}, and writing powers between 8 m W and 50 mW. As the structure is larger than the field of view of the writing microscope objective, several printing fields with a size of 420 × 420 µm^2 are stitched together, with an overlap region of 60 µm. Fabrication of the 1 cm^2-sized area takes approximately 10 h. After polymerization, the remaining liquid photoresist is removed in a bath of mr-dev 600 (Micro Resist Technology GmbH) for 20 min, followed by 3 min of isopropyl alcohol and subsequent drying with nitrogen.

The topography of the 3D-printed axicon is characterized quantitatively using confocal microscopy. Here, the measured topography is illustrated in Fig. 2(a), where a clean radially symmetric blazed grating with excellent linearity highlights the accuracy of the grayscale lithography. The structured surface is measured using a Nanofocus µSurf expert (NanoFocus AG) equipped with a 20× magnification, 0.6 NA objective. We chose a 7 nm *z*-pitch for the best resolution. The profile along the *y*-axis of the print plotted in Fig. 2(b) has a great overlap with the target design in Fig. 1(c), with steep 2π-phase jumps that excellently meet z_{max}. As the DOE is stitched together by lots of overlapping writing fields, some artifacts can be expected. Those stitching lines run exactly along the central x- and y-line of the topography plotted in Fig. 2(a) and are visible to some degree, though small in physical height. As two-photon polymerization 3D-printed optics are usually utilized in low-power applications such as imaging or quantum technologies, an investigation of the laser-induced damage threshold (LIDT) of the photoresist is necessary before any material processing can be performed. Although there has been a recent study of LIDT for these photoresists [32], and a performance investigation of 3D-printed microoptics within an optical cavity [33] for continuous wave laser operation, the laser pulse parameters used within are not comparable to those in this work. We perform LIDT testing with the ablation fluence threshold measurement method adapted from Liu [31]. A TRUMPF TruMicro series 6000 laser with a wavelength of 1030 nm, a pulse length of 3ps, and a repetition rate of 250 kHz ablates lines in multiple passes with width D from the IP-S photoresist with varying pulse energies. For LIDT testing of the photoresist IP-S, a sample printed on a two-inch fused-silica wafer is prepared, measuring one inch in diameter and having a thickness of 5 µm replicating the conditions of the axicon DOE in z_{max} and printing parameters. In Fig. 2(c), we plot D^2 for increasing pulse energies E_p with microscope images of three ablated lines with width D illustrated on graph's right-hand side. To determine the LIDT, D^2 is fitted linearly as a function of $\log_{10} E_p$. The threshold energy E_{th} is obtained from the extrapolation to $D^2 = 0$, and the corresponding threshold fluence is calculated from $F_{th} = 2E_{th}/\left(\pi w_0^2\right)$ [31]. Here, $E_{p,threshold} = 15.6 \pm 0.3$ µJ is the determined threshold pulse energy necessary for ablation, at waist radius $w_0 = (29.2 \pm 0.7)$ µm. This results in a fluence threshold of $1.17 \pm 0.02 J/cm^2$ at 3 ps, suitable for various laser materials processes, including in-volume modifications of transparent media. To put this value into perspective, we measured the LIDT of the pure fused-silica substrate with the same technique [31] and identical laser parameters; and achieved a threshold of $1.29 \pm 0.14 J/cm^2$ at 3 ps, allowing the use of 3 D-printed optics in high-intensity and high-average power laser-based materials processing at wavelengths around 1 µm.

Since the DOE's shape accuracy closely aligns with the design specifications, we expect corresponding beam-shaping performance, which is presented with Fig. 3. From the measured caustic of the Bessel-Gaussian beam, we extract profile cuts along x-z- and y-z-plane, respectively. The inset in Fig. 3 illustrates the transverse intensity x-y-plane at the z-position of highest intensity. The focus distribution is radially symmetric, creating a Bessel-Gaussian beam with a $1/e^2$-length of about 420 µm in air (650 µm in glass). The focus diameter is determined from the distance of the first zeros of the Bessel-like function [34], resulting in a 2 µm focal spot. This diameter also confirms operation at the diffraction limit given the employed wavelength and NA. Slight inhomogeneities in the intensity distribution can stem from stitching artifacts from the fabrication process of the DOE. Given these beam characteristics, the 3D-printed axicon DOE produces a Bessel–Gaussian beam with an aspect ratio above 300 (in glass), ideal for confined in-volume energy deposition in display glass substrates.

As next step, we induce full-thickness, in volume modifications in Corning Gorilla Glass 3 with a thickness of 550 µm using the 3D-printed axicon DOE shaping picosecond pulses from a TRUMPF TruMicro series 6000 laser with a wavelength of 1030 nm, a pulse duration of 3ps, a repetition rate of 10 kHz, and burst pulse energies of 150 µJ with four subpulses in the burst. Due to the high spatio-temporal photon density of the structured ultrashort laser pulses, a multi-photon absorption is induced, resulting in the formation of voids (type-III-regime modifications) [35] along the entire substrate thickness orthogonal to the surface [11]. The relative movement of the workpiece and the processing optics, cf. Figure 1(b), is achieved with a 2D axis stage with feed rates of 30 mm/s (For this preliminary study, we did not drive at maximum speed, nor did we use the laser at full power/energy). After inducing the modifications in the volume of the glass using the Bessel-like beam, a second step, the actual separation, is required [11]. Separation is required as the material is only precisely modified (or weakened), but no material is ejected as would be during laser ablation. Here, we apply the two most common techniques: thermal separation with a CO_2 laser [36] and selective laser etching (SLE) [5]. A smartphone-like display geometry separated thermally by a CO_2 laser (average power 15W, wavelength 10.6 µm, spot dimension ~2 mm) is illustrated in Fig. 4(a), demonstrating the capability of the presented approach to cut complex outer contours with laser-only machining [36].

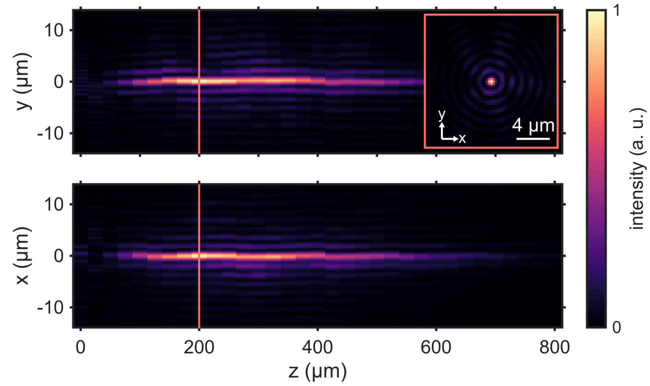

Fig. 3. Laser beam characterization of the Bessel-Gaussian beam generated with the 3D-printed axicon DOE at the design wavelength of 1030 nm in the x-z- (top) and y-z-plane (bottom). The inset shows the transverse intensity distribution at the position of the highest intensity, marked by the solid line.

Complex inner-counters (mm-scaled vias) separated by SLE (30 wt.-% KOH solution) are depicted in Fig. 4(b) [37]. Here, we demonstrate the possibility for more intricate glass geometries such as undercuts or cavities that can, for example, be applied to microfluidics. We additionally measure the topography of the glass edge as separated by the CO_2 laser via confocal microscopy (Nanofocus µSurf expert, with a 50×, 0.95 NA objective and 7 nm z-pitch). The topography is plotted in Fig. 4(c), with a surface roughness S_a of about 800 nm, similar to the state-of-the-art for glass cutting using ultrashort pulsed lasers [7].

To conclude, we have demonstrated that optical elements that are 3D-printed via two-photon polymerization can be used for laser materials processing. As an exemplary application scenario, glass cutting using ultrashort pulsed lasers with an elongated focus distribution was chosen. Here, a 3D-printed, square-centimeter-scaled diffractive axicon acts as a central beam shaping element, generating a Bessel-Gaussian beam that enables full-thickness, single-pass glass modifications. This printed component performs very similarly to glass optics in terms of shape accuracy, efficiency, processing result, etc., yet was manufactured within hours. Remarkably, with ~1 J/cm^2, the

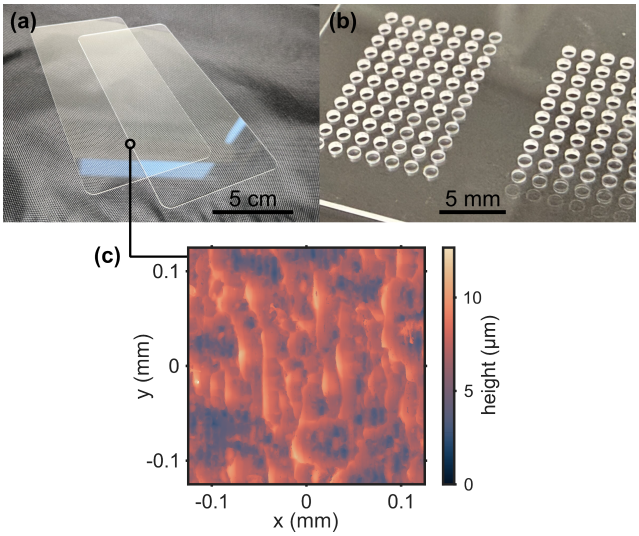

Fig. 4. Separation of the ultrashort pulse-modified Corning Gorilla Glass 3 via (a) thermal heating with a CO_2 Laser and (b) selective laser etching. (c) Confocally measured topography of the glass edge highlighted in (a).

threshold of the laser-induced damage tests using picosecond pulses at 1 µm wavelength is very close to that of fused-silica glass. We have, thus, found a fabrication concept that allows for rapid prototyping of customized optics that may contribute to developing new high-power laser machining strategies or to optimizing existing ones. In the future, additional LIDT and long-term exposure tests could help solidify the technology within the photonics sector.

Funding. European Innovation Council (IV-Lab: 101115545); European Research Council (3DPRINTEDOPTICS: 862549); European Regional Development Fund (project FEIH_FG2698214); Bundesministerium für Forschung, Technologie und Raumfahrt (Integrated3DPrint 13N16874, QLink.X, QR.X, QR.N); Deutsche Forschungsgemeinschaft (DFG-UP31/1, 431314977/GRK 2642, INST 41/1234-1); Ministerium für Wissenschaft, Forschung und Kunst Baden-Württemberg (Innovation Campus Future Mobility: ICM SdManu1, ICM Lab7, ICM Demo22); Baden-Württemberg Stiftung (OPTERIAL); Carl Zeiss Foundation (Center Qphoton, Endo-Print3D).

Acknowledgment. The authors thank Jonas Herbig for photographing the 3D-printed axicon DOE.

Disclosures. Leander Siegle, Daniel Flamm, and Harald Giessen are inventors on a pending patent covering aspects of the technology described in this work. The authors declare no further conflicts of interest.

Data availability. Data underlying the results presented in this paper are not publicly available at this time but may be obtained from the authors upon reasonable request.

REFERENCES

1. J. D. Majumdar and I. Manna, Int. Mater. Rev. **56**, 341 (2011).
2. H. Hügel, *Strahlwerkzeug Laser: Eine Einführung* (Springer-Verlag, 2013).
3. K. Sugioka and Y. Cheng, Light. Sci. Appl. **3**, e149 (2014).
4. M. Möller, P. Haug, P. Scheible, *et al.*, J. Laser Appl. **34**, 042015 (2022).
5. D. Flamm, M. Kaiser, M. Feil, *et al.*, J. Laser Appl. **34**, 012011 (2022).
6. M. Blothe, J. Joseph, M. Chambonneau, *et al.*, Opt. Lett. **50**, 6650 (2025).
7. D. Flamm, D. G. Grossmann, M. Sailer, *et al.*, Opt. Eng. **60**, 025105 (2021).
8. C. Mauclair, B. Najih, V. Comte, *et al.*, Opto-Electron. Sci. **4**, 250002 (2025).
9. V. V. Belloni, A.-M. Seydoux-Guillaume, S. Sao-Joao, *et al.*, Opt. Mater. Express **15**, 2460 (2025).
10. J. Hellstern, C. Tillkorn, T. Hieronymus, *et al.*, in *High-Power Laser Materials Processing: Applications, Diagnostics, and Systems XIII*, vol. **12878** (SPIE, 2024), p. 1287802.
11. M. Jenne, D. Flamm, K. Chen, *et al.*, Opt. Express **28**, 6552 (2020).
12. F. Wyrowski, H. van Esdonk, R. J. Zuidema, *et al.*, in *Diffractive and Holographic Optics Technology*, vol. **2152** (SPIE, 1994), p. 139.
13. C. Wahl, C. Grossert, D. Dung, *et al.*, in *High-Power Laser Materials Processing: Applications, Diagnostics, and Systems XIV*, vol. **13356** (SPIE, 2025), p. 23.
14. R. Brunner, R. Steiner, H.-J. Dobschal, *et al.*, in *Lithographic and Micromachining Techniques for Optical Component Fabrication II*, vol. **5183** (SPIE, 2003), p. 47.
15. E. Goi, X. Chen, Q. Zhang, *et al.*, Light. Sci. Appl. **10**, 40 (2021).
16. H. Ren, J. Jang, C. Li, *et al.*, Nat. Commun. **13**, 4183 (2022).
17. C. A. Richards, C. R. Ocier, D. Xie, *et al.*, Nat. Commun. **14**, 3119 (2023).
18. L. Siegle, D. Xie, C. A. Richards, *et al.*, Opt. Express **32**, 35678 (2024).
19. E. Skliutas, G. Merkininkaitė, S. Maruo, *et al.*, Nat. Rev. Methods Primers **5**, 15 (2025).
20. T. Aderneuer, O. Fernández, and R. Ferrini, Opt. Express **29**, 39511 (2021).
21. L. Siegle, S. Ristok, and H. Giessen, Opt. Express **31**, 4179 (2023).
22. J. Weinacker, S. Kalt, P. Kiefer, *et al.*, Adv. Funct. Mater. **34**, 2309356 (2024).
23. P. Kiefer, V. Hahn, S. Kalt, *et al.*, Light. Adv. Manuf. **4**, 1 (2024).
24. S. Wagner, L. Siegle, S. Haeusler, *et al.*, Adv. Opt. Mater. **13**, e02089 (2025).
25. K. Weber, S. Thiele, M. Hentschel, *et al.*, Adv. Quantum Technol. **7**, 2400135 (2024).
26. C.-X. Li, Y.-Q. Liu, D.-D. Han, *et al.*, Nat. Commun. **16**, 11513 (2025).
27. A. Rykov, I. Asharchuk, D. Obydennov, *et al.*, J. Micromechanics Micro Eng. **35**, 105005 (2025).
28. R. Horvat, L. Siegle, L. Schmid, *et al.*, Opt. Lett. **51**, 933 (2026).
29. J. Leach, G. M. Gibson, M. J. Padgett, *et al.*, Opt. Express **14**, 5581 (2006).
30. M. Schmid, D. Ludescher, and H. Giessen, Opt. Mater. Express **9**, 4564 (2019).
31. J. M. Liu, Opt. Lett. **7**, 196 (1982).
32. S. Klein, P. Ruchka, T. Klumpp, *et al.*, Opt. Mater. Express **13**, 3653 (2023).
33. S. Angstenberger, P. Ruchka, M. Hentschel, *et al.*, Opt. Lett. **48**, 6549 (2023).
34. D. McGloin and K. Dholakia, Contemp. Phys. **46**, 15 (2005).
35. K. Itoh, W. Watanabe, S. Nolte, *et al.*, MRS Bull. **31**, 620 (2006).
36. M. Kaiser, J. Kleiner, J. Wolff, *et al.*, in *Frontiers in Ultrafast Optics: Biomedical, Scientific, and Industrial Applications XXIV*, vol. **12875** (SPIE, 2024), p. 61.
37. M. Kaiser, M. Kumkar, R. Leute, *et al.*, in *Laser Applications in Microelectronic and Optoelectronic Manufacturing (LAMOM) XXIV*, vol. **10905** (SPIE, 2019), p. 19.